

Alma Mater Studiorum Università di Bologna  
Archivio istituzionale della ricerca

Testing the impact of discoplasty on the biomechanics of the intervertebral disc with simulated degeneration:  
An in vitro study

This is the final peer-reviewed author's accepted manuscript (postprint) of the following publication:

*Published Version:*

Techens C., Palanca M., Eltes P.E., Lazary A., Cristofolini L. (2020). Testing the impact of discoplasty on the biomechanics of the intervertebral disc with simulated degeneration: An in vitro study. MEDICAL ENGINEERING & PHYSICS, 84, 51-59 [10.1016/j.medengphy.2020.07.024].

*Availability:*

This version is available at: <https://hdl.handle.net/11585/808871> since: 2021-02-27

*Published:*

DOI: <http://doi.org/10.1016/j.medengphy.2020.07.024>

*Terms of use:*

Some rights reserved. The terms and conditions for the reuse of this version of the manuscript are specified in the publishing policy. For all terms of use and more information see the publisher's website.

This item was downloaded from IRIS Università di Bologna (<https://cris.unibo.it/>).  
When citing, please refer to the published version.

(Article begins on next page)

This is the final peer-reviewed accepted manuscript of:

**Med Eng Phys. 2020 Oct;84:51-59. doi:  
10.1016/j.medengphy.2020.07.024. Epub 2020 Jul 30.**

**Testing the impact of discoplasty on the biomechanics of the  
intervertebral disc with simulated degeneration: An in vitro study**

Chloé Techens, Marco Palanca, Peter Endre Éltés, Áron Lazáry, Luca  
Cristofolini

PMID: 32977922 DOI: 10.1016/j.medengphy.2020.07.024

The final published version is available online at:

<https://doi.org/10.1016/j.medengphy.2020.07.024>

Rights / License:

The terms and conditions for the reuse of this version of the manuscript are specified in the publishing policy. For all terms of use and more information see the publisher's website.

# **Testing the impact of discoplasty on the biomechanics of the intervertebral disc with simulated degeneration: an *in vitro* porcine study**

Chloé Techens, MEng <sup>1</sup>, Marco Palanca, Ph.D. <sup>1</sup>, Peter Endre Eltes MD <sup>2</sup>,  
Aron Lazary PhD <sup>2</sup>, Luca Cristofolini, Ph.D. <sup>1</sup>

<sup>1</sup> Department of Industrial Engineering, School of Engineering and Architecture, Alma  
Mater Studiorum - Università di Bologna, Bologna, Italy

<sup>2</sup> R&D Department of National Center for Spinal Disorders, Budapest, Hungary

***Submitted to:* Medical Engineering & Physics, special issue “Biomechanics for in silico clinical trials: thematic symposium of the IX Meeting of the Italian Chapter of the European Society of Biomechanics”**

***Original submission:*** 4<sup>th</sup> March 2020

***Revised version:*** 18<sup>th</sup> July 2020

## ***Statistics:***

Word count (manuscript):	@ 4890 words
Word count (abstract):	@ 238 words
Figures:	@ 9
Tables:	@ 2
References:	@ 43

## ***Corresponding author:***

Luca Cristofolini  
Department of Industrial Engineering  
School of Engineering and Architecture  
University of Bologna  
Viale Risorgimento, 2  
40136 Bologna, Italy  
e-mail: [luca.cristofolini@unibo.it](mailto:luca.cristofolini@unibo.it)

## 1    **ABSTRACT**

2    Percutaneous Cement Discoplasty has recently been developed to relieve pain in highly  
3    degenerated intervertebral discs presenting a vacuum phenomenon in patients that  
4    cannot undergo major surgery. Little is currently known about the biomechanical effects  
5    of discoplasty. This study aimed at investigating the feasibility of modelling empty discs  
6    and subsequent discoplasty surgery and measuring their impact over the specimen  
7    geometry and mechanical behavior. Ten porcine lumbar spine segments were tested in  
8    flexion, extension, and lateral bending under 5.4 Nm (with a 200 N compressive force  
9    and a 27 mm offset). Tests were performed in three conditions for each specimen: with  
10    intact disc, after nucleotomy and after discoplasty. A 3D Digital Image Correlation  
11    (DIC) system was used to measure the surface displacements and strains. The posterior  
12    disc height, range of motion (ROM), and stiffness were measured at the peak load. CT  
13    scans were performed to confirm that the cement distribution was acceptable.  
14    Discoplasty recovered the height loss caused by nucleotomy ( $p=0.04$ ) with respect to  
15    the intact condition, but it did not impact significantly either the ROM or the stiffness.  
16    The strains over the disc surface increased after nucleotomy, while discoplasty  
17    concentrated the strains on the endplates. In conclusion, this preliminary study has  
18    shown that discoplasty recovered the intervertebral posterior height, opening the  
19    neuroforamen as clinically observed, but it did not influence the spine mobility or  
20    stiffness. This study confirms that this *in vitro* approach can be used to investigate  
21    discoplasty.

## 22    **Keywords:**

23    Percutaneous Cement Discoplasty, Spine, Biomechanical testing, Strain

## 1. INTRODUCTION

Intervertebral Disc (IVD) degeneration is one of the main causes of low back pain, a large socio-economic burden for society, affecting between 60% and 70% of the population in industrialized countries at least once during their lifetimes [1]. Interbody fusion with the insertion of an intervertebral spacer after performing disc fenestration is the most common surgical treatment and has been widely studied in the literature [2]–[10]. It requires an invasive surgery which lasts for hours and is often associated with significant blood loss, long recovery, and general anaesthesia which is not suitable for elderly patients or those with significant comorbidities. Since this disease appears with age, finding minimally invasive treatments is crucial to treat the most complex cases. Percutaneous Cement Discoplasty (PCD), a surgical technique that minimizes the surgical morbidity and complication risks, is applied when a vacuum phenomenon is observed inside the IVD, resulting in the collapse of the adjacent vertebra and in nerve root compression. It consists of injecting an polymethylmethacrylate cement (PMMA) to “create individually shaped “in-site” intervertebral spacers” in order to recover the disc height and decompress the spinal canal [11]. One advantage of using PMMA to stabilize the spine is that “the load-bearing surface of the implant is fully adapted to the shape of the endplates”.

PCD is a newly developed technique, the authors found very little literature on the subject. Varga *et al* presented in 2015 the technique and their clinical study on 47 patients showed significant improvement in their quality of life, correlating with a pain factor decrease at 6 month follow-up [11]. Another study reported the surgery of a patient treated with PCD [12]. Discoplasty was shown to positively affect the spinal alignment and neuro-foraminal height in 27 patients [13].

While the impact of PCD on spine has been clinically assessed by comparing pre-operative/post-operative scores, no indication about spine kinetics and kinematics has been found by the authors. Some studies investigated similar techniques on animals, performing *in vitro* testing of spines in intact condition (with a full IVD), after removal of the Nucleus Pulposus (NP), and/or after a stabilization surgery. Refilling of the disc with soft materials [14] to recover intact spine mechanics was also investigated,

however it differs from discoplasty which uses acrylic cement. Only Moissonier *et al* and Wilke *et al* mimicked the PCD technique, implanting a spacer within the empty disc. The first demonstrated that nucleotomy of canine IVD increased the Range of Motion (ROM) and reduced disc height, whereas the presence of a hard mass inside the disc recovered the height loss but left ROM as wide as after nucleotomy [3]. The second attested that bone cement stabilized cervical discs, reducing the ROM compared to an intact spine [15]. Moreover, using animal surrogates usually limits access to naturally degenerated discs, consequently research has also focused on the best technique to model the vacuum phenomenon [16], [17], and the mechanical consequences of that surgery [18], [19]. In conclusion, PCD surgery relies on a weak knowledge of the mechanics of lumbar spine treated this way.

This study aims at enlarging knowledge about the mechanical consequences of PCD on lumbar spine stability. The motivations were two-fold: first, to develop a method to artificially represent a vacuum disc and the surgical technique applied to *in vitro* specimens, and to check the efficiency of this method as a model of PCD. Secondly, the study aimed at developing a methodology assessing the biomechanics of the spine before and after discoplasty. In particular, we hypothesized that PCD would recover the posterior disc height, affect the mechanical behaviour of the spine and present a damage risk for the surrounding tissue due to cement presence.

## **2. MATERIALS AND METHODS**

### **2.1. Specimens**

Ten functional spinal units were transected between T13 and L6 from porcine (*sus scrofa domestica*) thoracolumbar spines. The animals were young and healthy porcine (approximately 9 months old and 100 kg) sacrificed for alimentary purposes. The specimens were cleaned using surgical tools: all soft tissues were carefully removed from the segment without damaging the vertebra, the facet joints and the intervertebral disc. In order to keep the natural kinetics of the segment while testing, the anterior, supraspinous and posterior ligaments were left intact. Each segment was aligned based on the disc orientation, using a six-degree-of-freedom clamp. Both segment extremities were potted with acrylic bone cement. Specimens were stored frozen at -20 °C between cleaning and testing phases and between the tests which has been proven not to affect significantly the segment biomechanics [20].

## 2.2. Surgical procedure

The purpose of the study is to develop a method to investigate the impact of PCD on the biomechanical behaviour of the spine by comparing IVD treated by this technique to degenerated and healthy IVDs. Thus, each specimen was tested in the three conditions sequentially:

- intact (INT) with a healthy IVD,
- after nucleotomy (NUCL) to simulate the instability of degenerated discs,
- after discoplasty (DP) (Fig. 1).

## 2.3. Nucleotomy

Since the porcine specimens were euthanized before reaching skeletal maturation, degenerated disc instability has been manually simulated by reproducing the vacuum inside of the disc. The specimens were thawed at room temperature. A square incision was performed with a scalpel blade in the annulus fibrosus on the latero-posterior side of the disc. The nucleus pulposus, easily identified due to its softness, was completely extracted through the excision with a curette. The endplates were shaved by scratching off the soft tissue until the surfaces felt smooth. This did not weaken the endplates, as no intravertebral leakage was observed during discoplasty. The size of the incision corresponded to the disc height. The specimens were frozen at -20 °C until testing.

## 2.4. Discoplasty

After being tested in degenerated conditions, the specimens were treated with discoplasty. For that, the specimens were thawed at room temperature. A high-viscosity radiopaque acrylic bone cement (10% BaSO<sub>4</sub>) (Tecres, Italy) was injected inside the disc through the incision. Because the empty IVD was no longer in tension, the segment was distracted/stretched during the injection to avoid an underestimation of the cement volume. After injection, the cement hardened for 30 min. The specimens were frozen at -20 °C until testing. In one specimen the facet joint was unintentionally damaged at the end of the last test: checking the test results in retrospect confirmed there was no artefact.

## 2.5. Mechanical testing

All the specimens underwent the same test conditions. In order to simulate *in vivo* kinetics of porcine spines, a load with offset was applied to simulate flexion, extension,

and lateral bending (the same side was selected for each specimen based on the possible damages made during the preparation). This simplified loading scenario was chosen as it allows reproducible simulation of a realistic loading scenario. In quadrupeds, the choice of a side is less significant than for humans since they do not have a predisposed limb side. The specimens were mechanically tested with a uniaxial servo-hydraulic testing machine (Mod. 8032, Instron, UK) operated in displacement control. The upper pot was rigidly fixed to the top of the testing machine while the other was loaded through a spherical joint moving along a rail (Fig. 1). Before testing, each specimen was thawed at room temperature and pre-conditioned applying a sinusoidal loading at 0.5 Hz for 20 cycles to minimize viscoelastic creep effect. Specimens were loaded at 5.4 Nm by applying 200 N with an offset of 27 mm. The loading ramp lasted 1 s then the maximum loading was maintained for 0.3 s and the specimen was unloaded. The cycle was repeated 6 times (Fig. 2). Three cycles were found to be sufficient for preconditioning the data in another study [21], further cycles being nearly identical. The same trend was observed in these tests. The loading conditions were selected within the range of biological conditions, similar to other past studies [7], [14], [22]–[25]. Besides, the selected load avoided specimen damage. Each test was repeated twice to prove the experiment repeatability. Data extracted from the last cycle of both runs were averaged for each specimen. Axial load and displacement were acquired by the DIC system connected to a load cell (100 kN) at 15 Hz. Additionally, to have a more reliable sequence, the data were recorded with an independent computational unit (PXI, Labview, National Instruments, Aus. Texas, US) at 500 Hz. Unfortunately, some of the former records were missing for the first tests. Loads were either interpolated to have more data or smoothed with a median filter depending of the acquisition frequency.

## **2.6. Displacement and strain with DIC**

For each test, the specimen surface has been studied using a Digital Image Correlation set-up in order to track its displacements and strains. This technique requires a high-contrast speckle pattern on the region of interest. Thus, a white-on-black speckle pattern was prepared on both the vertebra and the intervertebral disc (Fig. 1). First, the segment was stained 3 times with a methylene blue solution to create a dark background without impacting the properties of the tissues [26]. The white pattern was then sprayed following a procedure optimized elsewhere [27]. To measure the displacements and the deformations over the specimen surface, a 3D-DIC system (Q400, Dantec Dynamics,



Skovlunde, Denmark) and the associated software (Instra 4D, v.4.3.1, Dantec Dynamics) were used. Images were acquired by two cameras (5 Megapixels, 2440 x 2050 pixels, 8-bit) with high-quality 35 mm lenses (Apo-Xenoplan 1.8/35, Schneider-Kreuznach, Bad-Kreuznach, Germany) inclined at an angle of 26° (white dot line on Fig. 1). The field of view covered the entire specimen (about 50mm by 30mm), which gave a pixel size of about 0.02mm. The specimen was lit by cold-light LEDs. Before the tests, calibration of the DIC system was performed using a dedicated target (A14-BMB-9x9, Dantec Dynamics). The parameters for the images acquisition and the correlation analysis have been previously optimized to minimize the error: facet size of 35 pixels, grid spacing of 11 pixels, and local filtering with a 7x7 pixels kernel. In order to investigate the biomechanical behaviour of the spine, two different acquisitions were performed:

- For extension and flexion: Lateral view of the segment with the cameras pointing at the neuroforamen
- For lateral bending; Frontal view of the specimen with the cameras pointing to the selected bending side

Images were taken at 15 Hz from the unloaded condition (reference frame, no load applied) to the end of the 6th cycle.

## **2.7. Data analysis and statistics**

The parameters were extracted from the last load cycle of each of the two repetitions of each loading configuration. All measurements were compared for each specimen between the three disc conditions: intact, nucleotomy, discoplasty. In order to assess the changes in the nerve space in the neuroforamen, which is the main point in doing discoplasty, the posterior disc height was measured using DIC images: one point on each endplate was identified on the 3D profile of the disc in the back of the disc, close to the neuroforamen, where the nerve is passing. The points were aligned in the cranial-caudal direction. Their position was therefore tracked using DIC software. As a result, posterior disc height was only computed in flexion and extension, the frontal view not allowing height computation in lateral bending.

Displacements of the caudal vertebra in relation to the cranial vertebra were calculated from DIC images with a Matlab script. Assuming vertebra to be rigid bodies, the motions (translations and rotations) of each vertebra were computed based on singular value

decomposition. The ROM was defined as the relative angle between the vertebra in the sagittal plane between the peak load and unloaded conditions.

A pilot study of the load-displacement curves determined that, for porcine spines, the position having a first derivative of 30 N/mm was at the limit of the laxity zone (LZ). Stiffness was defined as the slope of load-displacement relationship in LZ. Although for some specimens this method underestimated the length of the LZ, the stiffness computation was not impacted since it was within the linear region [28].

All the computations were performed with dedicated Matlab scripts (Mathworks, Inc., Natick, MA, USA). All height and strain measurements were evaluated by two independent observers. To limit inter-specimen variability influence, all stiffnesses, heights, and ROMs values were normalized to the intact condition.

In addition to posterior disc height, ROM, and stiffness calculations, the true principal strains over the specimen surface (vertebra and IVD) were measured at the peak load. In particular, the disc surface area was manually identified and the minimum, maximum and average of the first and second principal strains were extracted. Those measurements were performed in flexion and extension because the frontal view did not allow consideration of the neuroforamen area.

For each parameter, outlying data were preliminarily tested and excluded using the Peirce criterion [29], this resulted in a 10% data exclusion at the maximum. Test parameters were computed based on the sixth cycle. Mean  $\pm$  standard deviation of all the outcomes were calculated and presented by group. Due to the small specimen number, comparisons between the three conditions were made for ROM, stiffness, height, and the strain average with a non-parametric test (Wilcoxon's sign rank, with Matlab).

## **2.8. Cement distribution**

In order to study the cement distribution inside of the disc, scans of the specimens have been performed after discoplasty with a clinical computed tomography scanner (Aquilion ONE, Toshiba) with 120 mA, 135 kV and a 0.5 mm voxel. The scans of nine specimens out of ten were available due to a practical mistake. The shape of the cement, its capacity to fill the disc cavity, the endplates and AF contact were visually assessed by a spine surgeon (P.E.) from the 3D reconstruction of the PMMA geometry. Segmentation process was performed in Mimics® image analysis software (Mimics

Research, Mimics Innovation Suite v21.0, Materialise, Leuven, Belgium) on the 2D CT images using thresholding algorithm.

### **3. RESULTS**

#### **3.1. Posterior disc height**

The posterior disc height was measured in the three conditions. At peak load, intact posterior disc height was higher in flexion than in extension. Nucleotomy significantly decreased the posterior height for both flexion ( $p=0.006$ , Wilcoxon) and extension ( $p=0.049$ , Wilcoxon) (Fig. 3). On the contrary, discoplasty restored the height. Results were normalized to the initial posterior height for each specimen. In extension, height after discoplasty was significantly higher (105% of the intact height) than after nucleotomy (81%) ( $p=0.04$ , Wilcoxon). In flexion, posterior disc height was respectively 84% and 94% of the intact height after nucleotomy and discoplasty but the difference between the two conditions was not significant ( $p=0.11$ , Wilcoxon).

#### **3.2. Range of motion**

Intervertebral motions in the applied direction were one order of magnitude higher compared to the other directions. Only the motions in the applied direction are reported here. In flexion and lateral bending, nucleotomy reduced the ROM (Fig. 4). The ROM in extension slightly increased after nucleotomy and discoplasty compared to the intact condition. The results for degenerated and discoplasty discs were normalized by the intact ROM for each motion. ROM was not significantly different between nucleotomy and discoplasty in flexion (Wilcoxon sign-rank test,  $p=0.57$ ), extension ( $p=0.43$ ) and lateral bending ( $p=0.50$ , Wilcoxon).

#### **3.3. Stiffness**

Stiffness was computed for only 9 out of 10 specimens due to a technical problem during acquisition. Specimens had very different behaviours regardless of the loading configuration and spinal level. The majority of the tests presented a “toe-region” before a stiff region. A recovery after discoplasty of the initial behaviour compared to after nucleotomy was also observed (Fig. 5). The results for nucleotomy and discoplasty discs were normalized by the intact stiffness for each loading configuration. Stiffness was not

significantly different after nucleotomy and discoplasty in flexion ( $p=0.47$ , Wilcoxon), extension ( $p=0.95$ , Wilcoxon) and lateral bending ( $p=0.46$ , Wilcoxon) (Fig. 6).

### **3.4. Strain distribution**

DIC correlation has been successfully performed in flexion and extension only because the frontal view did not allow all of the disc surface to be captured. First of all, bone strains were in a  $[-1.5\%, 1.5\%]$  range on the vertebra surface whereas they reached  $-17\%$  and  $+11\%$  on the discs. Moreover, IVD principal strains presented different behaviours depending on the loading configuration (Fig. 7). In flexion, for all disc conditions, the highest values of compressive strain are located at the cranial and caudal extremities of the IVD, starting from the anterior and spreading toward the posterior along the endplates. After nucleotomy and discoplasty, the trend was more pronounced. However, cemented discs presented lower values in this area than empty discs. The highest values of tensile principal strain were in the centre of the IVD with peak  $>3\%$  of strain in the posterior region. In extension, tensile strains were larger in the anterior of the disc while high compressive strains were located in the posterior area of the disc. Discoplasty reduced the strains in most of the disc, whereas for intact and nucleotomy, high strains were found on the whole disc.

Nucleotomy seems to have a greater effect on the compressive strain in flexion and extension (Table 1). Meanwhile, discoplasty halved the average tensile strain of disc surface compared to nucleotomy condition in extension ( $p=0.0195$ , Wilcoxon) but had similar values of second principal strain. Regarding the peak strains, discoplasty only presented a value larger than intact condition for extension. Other extreme strains were observed after nucleotomy although the differences were not significant.

### **3.5. Cement distribution**

Nine specimens have been scanned to control cement distribution within the discs. Visual assessment of the specimen scans focused on the position of the cement mass within the intervertebral disc in the sagittal and frontal planes, whether it was in contact with endplates and AF, the shape of the distribution, and the ratio of disc filling. The majority of specimens had a cement volume located in the posterior of the disc (9/9 specimens), centred in the lateral direction (8/9 specimens), in contact with the endplates

(8/9). Only two specimens did not present contact between the cement and the AF (Fig. 8). The NP cavity was fully filled with cement in 5 specimens, three discs were almost filled at >80% of the NP volume, and one at less than 80%. Among the specimens, seven were validated by a clinician as discoplasty models compared to cement distribution after human surgery taking porcine anatomical specificities into account, and two were sub-optimal (Fig. 9). No outlier corresponded to the sub-optimal cemented specimens. All specimens presented a smaller cement volume than in human surgery (Table 2).

#### 4. DISCUSSION

According to clinical observations [11], a loss of disc height due to disc degeneration would result in a reduction of the neuroforamen where the back nerves are passing, compressing them and creating pain for the patient. This animal *in vitro* study aimed at exploring the feasibility of assessing the mechanical consequences on spine stability after discoplasty surgical procedure. An *in vitro* experiment was successfully conducted to establish posterior disc height, ROM, stiffness, and strains over porcine specimen surfaces.

After nucleotomy a decrease of the posterior disc height of 15% was measured. This result validated such *in vitro* nucleotomy as a simulation of degenerated disc. Furthermore, nucleotomy was associated with a decrease of ROM (not statistically significant in our sample). After discoplasty, the injected cement acted like a spacer resulting in a significant recovery of the posterior height (105% of the intact height in extension). This trend supported the clinical observations [11] and confirmed that PCD recovered the disc height and enlarged neuroforamen space, which is the main objective of this surgery. ROM and stiffness did not show any significant difference between the degenerated and treated cases for any loading. Thus, discoplasty did not significantly impact spine flexibility in this experimental setup.

To the authors' knowledge, this was the first study addressing the consequences of discoplasty on the distribution of strain on the disc surface. The strain distribution measured after nucleotomy showed a specific pattern with intense regions, while discoplasty reduced this abnormal distribution with more moderate strain values.

DIC results showing the AF principal strains can be related to the ROM and the posterior disc height. After nucleotomy, because of the reduced posterior height and because the annulus is no longer constrained from inside, the annulus fibres bulged more, leading to

intense tensile strains at the apex of the bulging. At the same time, this more pronounced bulging at mid-height caused a more pronounced concavity at the disc cranial and caudal extremities, which led to larger compressive strains in this region. After discolplasty, the injected cement spaced the endplates, and even if the cement did not stretch radially the disc fibres as the NP would do, the overall bulging was more limited, and less intense tensile strains were measured. As the cement acts as a very stiff spacer, very small strains were visible in most of the disc surface, the only highly strained region in the disc was near the endplates. Strain values after discolplasty did not exceed what the endplates underwent in nucleotomy condition. If the specimen endplates presented any weakness, this could lead to long-term damages due to the load concentration. The peak strain values increased after nucleotomy, and decreased again after cement injection, reaching intact-like values. No correlation between the strain peaks on the specimen surface and the cement distribution assessed from the CT scans was found. Even in the specimens where contact between the AF and the cement was noted, this did not result in a specific strain distribution.

The ROM measured at peak load was in the same range as other *in vitro* studies on porcine lumbar spines [22], [30]. Others studies investigating the effect of nucleotomy demonstrated that the absence of NP reduced segmental rotational stability, significantly increasing the ROM [14], [19], [23].

Discolplasty being a recent surgical technique, the authors found only one article applying a similar surgery, on dog cervical discs [3]: nucleotomy was also performed through an AF fenestration and a spacer implant was inserted. Similar to the present study, Moissonier *et al* found that nucleotomy completely disrupted spine stability, increasing significantly the ROM. Both the spacer used in their study, and the cement injected in ours failed to recover disc mobility. Similarly, the cement set in the cervical disc by Wilke *et al* reduced the ROM compared to intact disc condition. However, this study tested bone cement to anticipate interbody fusion, and the AF was not fully intact [15]. This was the major difference with soft disc filler materials which are more likely to restore intact ROM as well [14].

Although the results were normalized with respect to the intact to integrate the specimen anatomical specificity, and one outlier was removed, inter-specimen variability remained large, with no correlation with the segment level. Our tests differed from most of the literature [28] as the FSUs were tested separately in flexion and extension, therefore direct comparisons of the stiffness are not possible.

This study aimed to start exploring the biomechanical effects of discoplasty. Since this is a preliminary study, an animal model was more justifiable for ethical reasons. The use of breed porcine rather than human spines was preferred as they have less inter-specimen variation of anatomy and mechanical properties. Indeed, porcine models are commonly used to replicate human spine surgeries [31], [32]. Porcine spines could be good surrogates for *in vitro* testing, even if they exhibit larger ROM and lower stiffness [33]–[35]. Since the porcine specimens were obtained before reaching skeletal maturity, finding IVDs presenting a similar degenerated level with a vacuum as required for PCD was impossible. Nucleotomy did not aim at modelling a degenerated disc state but at creating the spine instability observed clinically based on the disc vacuum. Porcine results should therefore be qualitatively extrapolated to humans in terms of trends rather than interpreting absolute values as this study aimed at.

Vacuum volume has not been measured in this study. The importance of this parameter is unclear in the clinical practice. A recent study investigating the Vacuum Phenomenon (VP) impact for PCD indication concluded that the volume of vacuum could not be used as a proper indication for this surgery [36]. Moreover, during the PCD procedure, the patient position aims at enlarging the intervertebral space by reducing the segmental lordosis. Thus, the volume of the empty disc available during the surgery is larger than the VP computed on imaging.

Usual methods to measure the disc height like Farfan or Frobin were not applied here to assess the intervertebral space. Indeed, these methods were conceived for clinical application considering the vertical height along the antero-posterior disc length on medical images, taking account of the whole disc and its orientation. This study, however, focused on the nerve space within the neuroforamen. Only the volume where the nerve passed was critical, based on clinical observations, and the discoplasty surgery was applied in first approach to re-open the foramen space by achieving indirect decompression. That is why a comparative study has been performed selecting two points at the endplates level the closest from the neuroforamen, rather than relying on a more general measurement of the disc height. The study concentrated on parameters with meaning for the clinical purpose of the surgery. Moreover, the most critical case was also investigated: physiologically when the disc is loaded in extension and the neuroforamen is the most reduced. So, measurements at the peak load were more interesting for the study.

The impact of AF fenestration during nucleotomy on the segment stability has not been assessed here, however Michalek *et al* reported alterations of IVD mechanics with disc height loss under a compressive load, following different types of incisions [37]. Disc lesions were also found to reduce the peak moment depending on the damage shape [38]. As a consequence, our study may overestimate motion range. However, it was hypothesized that the lack of NP would destabilize the segment in larger proportion than the fenestration of AF.

Pure moment is the gold-standard loading for *in vitro* spine testing in a relevant bending condition. For spine segments consisting of several vertebrae, bending is usually associated with a follower load equipment to model the *in vivo* kinematics, including the effect of the muscles adding a compressive loading [39], [40]. Similarly, a compressive preload is found in a single FSU, but in this case a follower load cannot be implemented. In this study, an alternative loading configuration was chosen to ensure that reproducible testing conditions could be applied, thus allowing the comparison of the biomechanics of a specimen tested at different times with each of the different disc conditions. The load applied here was a combination of axial compression and bending, an alternative loading to pure bending of the spine [26], [41]–[44]. It has been demonstrated that without preload, *in vivo* stiffness of the spine segment was underestimated applying pure bending [45]. In our study, the combination of axial compression and bending allowed a more physiological spine loading with an axial component which substitutes of the preload.

## 5. CONCLUSION

So far, the only knowledge about PCD comes from clinical experience on few cases. This paper presents a feasibility study, to develop a test model and perform a preliminary investigation on the biomechanics of PCD. The study also aimed at analyzing and verifying if there is any clear mechanical risk associated with injection of cement in the cavity of a disc. No specific clinical recommendations (e.g. indication for specific patient groups) can be directly obtained from the present study. This study aimed at developing an *in vitro* surrogate to test a highly degenerated disc with vacuum inside, and to assess the biomechanical changes related to discoplasty in porcine spines. The main conclusions could be summarized in key points.



- The *in vitro* method was successfully developed to model nucleotomy.
- The *in vitro* testing protocol applied to discoplasty allowed to measure the effect of this minimally invasive surgery on the spine biomechanics.
- Nucleotomy decreased the posterior disc height. Discoplasty restored the height significantly, maintaining a gap between the vertebral bodies and re-opening the neuroforamen area as observed in clinical practice.
- The CT scans confirmed that the distribution of the cement had a similar distribution inside the disc for most specimens compared to human post-surgery observations, although the cavity after nucleotomy and the cement volume were smaller than in human cases.
- Discoplasty did not impact the ROM nor the stiffness, which remained similar to the nucleotomy condition because the cement did not directly interact with the AF nor the facets.
- Discoplasty concentrated the strains along the endplates, reducing the strain value on the middle of the disc. The average strain over the disc was decreased after discoplasty compared to nucleotomy, limiting the risks of fibre tears.
- The goal of this preliminary study on a limited number of porcine specimens was to establish trends which could justify a larger study on human specimens.

## Acknowledgments

The Authors wish to thank Federico Morosato from the University of Bologna for providing the Matlab scripts.

Villalba Hospital is acknowledged for hosting the scan sessions; special thanks to Pierangela Moro for the skilled advice and for her great patience.

Special thanks are expressed to Cameron James, ESR within the Spinner project, for proof-reading the manuscript.

The use Mimics Software was possible thanks to the Hungarian Scientific Research Fund (OTKA FK123884).

This project was founded by European Union's Horizon 2020 Marie Skłodowska-Curie ITN grant SPINNER No. 766012.

432 **Conflict of interest statement**

433 There is no potential conflict of interest: none of the Authors received or will receive  
434 direct or indirect benefits from third parties for the performance of this study.

435

## 436 REFERENCES:

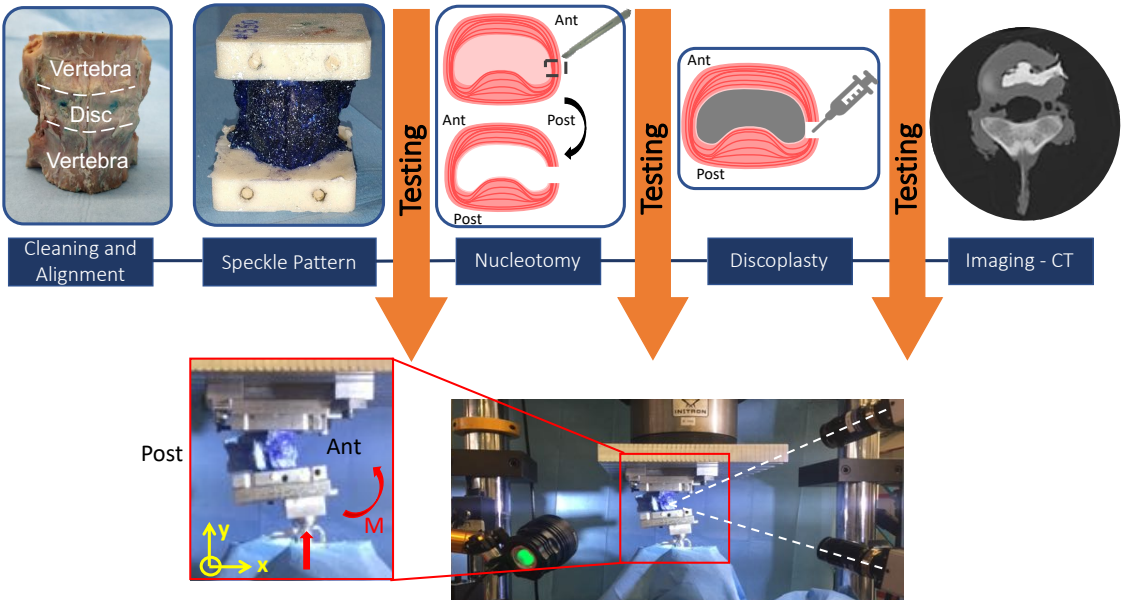
- 437 [1] « 6. Priority diseases and reasons for inclusion », in *WHO | Priority Medicines*  
438 *for Europe and the World Update Report*, 2013.
- 439 [2] I. Oda, K. Abumi, B.-S. Yu, H. Sudo, et A. Minami, « Types of Spinal Instability  
440 That Require Interbody Support in Posterior Lumbar Reconstruction: An In Vitro  
441 Biomechanical Investigation. [Miscellaneous Article] », *Spine*, vol. 28, n° 14, p.  
442 1573-1580, juill. 2003.
- 443 [3] P. Moissonnier, L. Desquilbet, D. Fitzpatrick, et F. Bernard, « Radiography and  
444 biomechanics of sixth and seventh cervical vertebrae segments after disc  
445 fenestration and after insertion of an intervertebral body spacer », *Vet. Comp.*  
446 *Orthop. Traumatol.*, vol. 27, n° 1, p. 54-61, 2014, doi: 10.3415/VCOT-11-11-  
447 0159.
- 448 [4] X. Li, Y. Song, et H. Duan, « Reconstruction of Segmental Stability of Goat  
449 Cervical Spine with Poly (D, L-lactic acid) Cage », *Orthop. Surg.*, vol. 7, n° 3, p.  
450 266-272, 2015, doi: 10.1111/os.12192.
- 451 [5] F. Kandziora, R. Pflugmacher, M. Scholz, T. D. Eindorf, K. J. Schnake, et N. P.  
452 Haas, « Bioabsorbable Interbody Cages in a Sheep Cervical Spine Fusion  
453 Model. », *Spine*, vol. 29, n° 17, p. 1845-1855, sept. 2004.
- 454 [6] F. Kandziora *et al.*, « Comparison of BMP-2 and combined IGF-I/TGF- $\beta$ 1  
455 application in a sheep cervical spine fusion model », *Eur. Spine J.*, vol. 11, n° 5,  
456 p. 482-493, oct. 2002, doi: 10.1007/s00586-001-0384-4.
- 457 [7] Y. Gu, Z. Yao, L. Jia, J. Qi, et J. Wang, « In vivo experimental study of hat type  
458 cervical intervertebral fusion cage (HCIFC) », *Int. Orthop.*, vol. 34, n° 8, p.  
459 1251-1259, déc. 2010, doi: 10.1007/s00264-010-0978-8.
- 460 [8] Z. Chunguang *et al.*, « Evaluation of Bioabsorbable Multiamino Acid  
461 Copolymer/ $\alpha$ -Tri-Calcium Phosphate Interbody Fusion Cages in a Goat Model »,  
462 *Spine*, vol. 36, n° 25, p. E1615-E1622, déc. 2011, doi:  
463 10.1097/BRS.0b013e318210ca32.
- 464 [9] M. J. Allen, Y. Hai, N. R. Ordway, C.-K. Park, B. Bai, et H. A. Yuan,  
465 « Assessment of a synthetic anterior cervical ligament in a spinal fusion model in  
466 sheep », *Spine J.*, vol. 2, n° 4, p. 261-266, juill. 2002, doi: 10.1016/S1529-  
467 9430(02)00188-2.
- 468 [10] S. E. Emery, D. A. Fuller, et S. D. Stevenson, « Ceramic Anterior Spinal Fusion:  
469 Biologic and Biomechanical Comparison in a Canine Model. [Miscellaneous  
470 Article] », *Spine*, vol. 21, n° 23, p. 2713-2719, déc. 1996.
- 471 [11] P. P. Varga, G. Jakab, I. B. Bors, A. Lazary, et Z. Szövérfi, « Experiences with  
472 PMMA cement as a stand-alone intervertebral spacer », *Orthop.*, vol. 44, n° 1, p.  
473 1-8, nov. 2015, doi: 10.1007/s00132-014-3060-1.
- 474 [12] C. Sola *et al.*, « Percutaneous cement discoplasty for the treatment of advanced  
475 degenerative disk disease in elderly patients », *Eur. Spine J.*, mars 2018, doi:  
476 10.1007/s00586-018-5547-7.
- 477 [13] L. Kiss, P. P. Varga, Z. Szoverfi, G. Jakab, P. E. Eltes, et A. Lazary, « Indirect  
478 foraminal decompression and improvement in the lumbar alignment after  
479 percutaneous cement discoplasty », *Eur. Spine J.*, avr. 2019, doi:  
480 10.1007/s00586-019-05966-7.
- 481 [14] H.-J. Wilke, F. Heuer, C. Neidlinger-Wilke, et L. Claes, « Is a collagen scaffold  
482 for a tissue engineered nucleus replacement capable of restoring disc height and  
483 stability in an animal model? », *Eur. Spine J.*, vol. 15, n° 3, p. 433-438, août  
484 2006, doi: 10.1007/s00586-006-0177-x.

- [15] H.-J. Wilke, A. Kettler, et L. Claes, « Primary stabilizing effect of interbody fusion devices for the cervical spine: an in vitro comparison between three different cage types and bone cement », *Eur. Spine J.*, vol. 9, n° 5, p. 410-416, oct. 2000, doi: 10.1007/s005860000168.
- [16] G. Vadalà *et al.*, « A Nucleotomy Model with Intact Annulus Fibrosus to Test Intervertebral Disc Regeneration Strategies », *Tissue Eng. Part C Methods*, vol. 21, n° 11, p. 1117-1124, 2015, doi: <http://dx.doi.org/10.1089/ten.tec.2015.0086>.
- [17] G. Vadalà *et al.*, « The Transpedicular Approach As an Alternative Route for Intervertebral Disc Regeneration », *Spine*, vol. 38, n° 6, p. E319-E324, mars 2013, doi: 10.1097/BRS.0b013e318285bc4a.
- [18] M. Shea, T. Y. Takeuchi, R. H. Wittenberg, A. A. White, et W. C. Hayes, « A Comparison of the Effects of Automated Percutaneous Discectomy and Conventional Discectomy on Intradiscal Pressure, Disk Geometry, and Stiffness », *J. Spinal Disord.*, vol. 7, n° 4, p. 317-325, août 1994, doi: 10.1097/00002517-199408000-00005.
- [19] W. Johannessen, J. M. Cloyd, G. D. O'Connell, E. J. Vresilovic, et D. M. Elliott, « Trans-Endplate Nucleotomy Increases Deformation and Creep Response in Axial Loading », *Ann. Biomed. Eng.*, vol. 34, n° 4, p. 687-696, avr. 2006, doi: 10.1007/s10439-005-9070-8.
- [20] J. S. Tan et S. Uppuganti, « Cumulative Multiple Freeze-Thaw Cycles and Testing Does Not Affect Subsequent Within-Day Variation in Intervertebral Flexibility of Human Cadaveric Lumbosacral Spine », *SPINE*, vol. 37, n° 20, p. E1238-E1242, 2012.
- [21] J. M. Cottrell, M. C. H. van der Meulen, J. M. Lane, et E. R. Myers, « Assessing the Stiffness of Spinal Fusion in Animal Models », *HSS J.*, vol. 2, n° 1, p. 12-18, févr. 2006, doi: 10.1007/s11420-005-5123-7.
- [22] J. P. Dickey et D. J. Kerr, « Effect of specimen length: are the mechanics of individual motion segments comparable in functional spinal units and multisegment specimens? », *Med. Eng. Phys.*, vol. 25, n° 3, p. 221-227, avr. 2003, doi: 10.1016/S1350-4533(02)00152-2.
- [23] F. Russo *et al.*, « Biomechanical Evaluation of Transpedicular Nucleotomy With Intact Annulus Fibrosus », *SPINE*, vol. 42, n° 4, p. E193-E201, févr. 2017, doi: 10.1097/BRS.0000000000001762.
- [24] D. J. Sucato, « Thoracoscopic Discectomy and Fusion in an Animal Model: Safe and Effective When Segmental Blood Vessels Are Spared. », *SPINE*, vol. 27, n° 8, p. 880-886, 2002.
- [25] Chung et Teoh, « Multi-axial Spine Biomechanical Testing System with Speckle Displacement Instrumentation », *J. Biomech. Eng.*, vol. 124, n° 4, p. 471-477, août 2002, doi: 10.1115/1.1493803.
- [26] M. Palanca, M. Marco, M. L. Ruspi, et L. Cristofolini, « Full-field strain distribution in multi-vertebra spine segments: An in vitro application of digital image correlation », *Med. Eng. Phys.*, vol. 52, p. 76-83, févr. 2018, doi: 10.1016/j.medengphy.2017.11.003.
- [27] M. Palanca, T. M. Brugo, et L. Cristofolini, « USE OF DIGITAL IMAGE CORRELATION TO INVESTIGATE THE BIOMECHANICS OF THE VERTEBRA », *J. Mech. Med. Biol.*, vol. 15, n° 02, p. 1540004, avr. 2015, doi: 10.1142/S0219519415400047.
- [28] H.-J. Wilke, K. Wenger, et L. Claes, « Testing criteria for spinal implants: recommendations for the standardization of in vitro stability testing of spinal

- implants », *Eur. Spine J.*, vol. 7, n° 2, p. 148-154, mai 1998, doi: 10.1007/s005860050045.
- [29] S. M. Ross, « Peirce's criterion for the elimination of suspect experimental data », *J. Eng. Technol.*, p. 1-12, 2003.
- [30] J. T. Lysack, J. P. Dickey, G. A. Dumas, et D. Yen, « A continuous pure moment loading apparatus for biomechanical testing of multi-segment spine specimens », *J. Biomech.*, vol. 33, n° 6, p. 765-770, juin 2000, doi: 10.1016/S0021-9290(00)00021-X.
- [31] Busscher, « Comparative anatomical dimensions of the complete human and porcine spine », 2010.
- [32] C. Daly, P. Ghosh, G. Jenkin, D. Oehme, et T. Goldschlager, « A Review of Animal Models of Intervertebral Disc Degeneration: Pathophysiology, Regeneration, and Translation to the Clinic », *BioMed Res. Int.*, vol. 2016, 2016, doi: 10.1155/2016/5952165.
- [33] H.-J. Wilke, J. Geppert, et A. Kienle, « Biomechanical in vitro evaluation of the complete porcine spine in comparison with data of the human spine », *Eur. Spine J.*, vol. 20, n° 11, p. 1859-1868, nov. 2011, doi: 10.1007/s00586-011-1822-6.
- [34] J. P. Dickey, G. A. Dumas, et D. A. Bednar, « Comparison of porcine and human lumbar spine flexion mechanics\* », *Vet. Comp. Orthop. Traumatol.*, vol. 16, n° 01, p. 44-49, 2003, doi: 10.1055/s-0038-1632753.
- [35] I. Busscher, A. J. van der Veen, J. H. van Dieen, I. Kingma, G. J. Verkerke, et A. G. Veldhuizen, « In Vitro Biomechanical Characteristics of the Spine A Comparison Between Human and Porcine Spinal Segments », *SPINE*, vol. 35, n° 2, p. E35-E42, janv. 2010, doi: 10.1097/BRS.0b013e3181b21885.
- [36] G. Camino Willhuber *et al.*, « Development of a New Therapy-Oriented Classification of Intervertebral Vacuum Phenomenon With Evaluation of Intra- and Interobserver Reliabilities », *Glob. Spine J.*, p. 2192568220913006, mars 2020, doi: 10.1177/2192568220913006.
- [37] A. J. Michalek et J. C. Iatridis, « Height and torsional stiffness are most sensitive to annular injury in large animal intervertebral discs », *Spine J.*, vol. 12, n° 5, p. 425-432, mai 2012, doi: 10.1016/j.spinee.2012.04.001.
- [38] R. E. Thompson, M. J. Percy, et T. M. Barker, « The mechanical effects of intervertebral disc lesions », *Clin. Biomech.*, vol. 19, n° 5, p. 448-455, juin 2004, doi: 10.1016/j.clinbiomech.2004.01.012.
- [39] A. G. Patwardhan, R. M. Havey, K. P. Meade, B. Lee, et B. Dunlap, « A Follower Load Increases the Load-Carrying Capacity of the Lumbar Spine in Compression. », *SPINE*, vol. 24, n° 10, p. 1003-1009, 1999.
- [40] A. G. Patwardhan, K. P. Meade, et B. Lee, « A Frontal Plane Model of the Lumbar Spine Subjected to a Follower Load: Implications for the Role of Muscles », *J. Biomech. Eng.*, vol. 123, n° 3, p. 212-217, juin 2001, doi: 10.1115/1.1372699.
- [41] M. A. Adams, S. May, B. J. C. Freeman, H. P. Morrison, et P. Dolan, « Effects of Backward Bending on Lumbar Intervertebral Discs: Relevance to Physical Therapy Treatments for Low Back Pain. », *SPINE*, vol. 25, n° 4, p. 431-437, 2000.
- [42] M. Al-Rawahi, J. Luo, P. Pollintine, P. Dolan, et M. A. Adams, « Mechanical Function of Vertebral Body Osteophytes, as Revealed by Experiments on Cadaveric Spines », *Spine*, vol. 36, n° 10, p. 770-777, mai 2011, doi: 10.1097/BRS.0b013e3181df1a70.

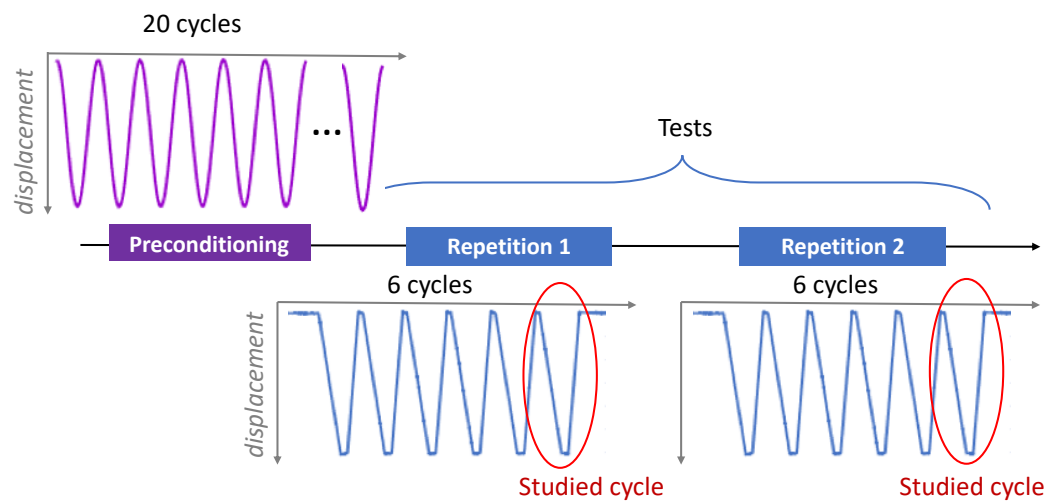
- 583 [43] M. L. Ruspi, M. Palanca, C. Faldini, et L. Cristofolini, « Full-field in vitro  
584 investigation of hard and soft tissue strain in the spine by means of Digital Image  
585 Correlation », *Muscles Ligaments Tendons J.*, vol. 7, n° 4, p. 538-545, avr. 2018,  
586 doi: 10.11138/mltj/2017.7.4.538.
- 587 [44] M. Adams et P. Dolan, « Time-dependent changes in the lumbar spine's  
588 resistance to bending », *Clin. Biomech.*, vol. 11, n° 4, p. 194-200, juin 1996, doi:  
589 10.1016/0268-0033(96)00002-2.
- 590 [45] M. G. Gardner-Morse et I. A. Stokes, « Physiological axial compressive preloads  
591 increase motion segment stiffness, linearity and hysteresis in all six degrees of  
592 freedom for small displacements about the neutral posture », *J. Orthop. Res.*, vol.  
593 21, n° 3, p. 547-552, janv. 2003, doi: 10.1016/S0736-0266(02)00199-7.  
594  
595

596 CAPTIONS TO FIGURES



597 **Fig. 1** – Experimental workflow of the study. The arrow represents the applied load  
598 and the resulting moment  $M$ .  
599

600

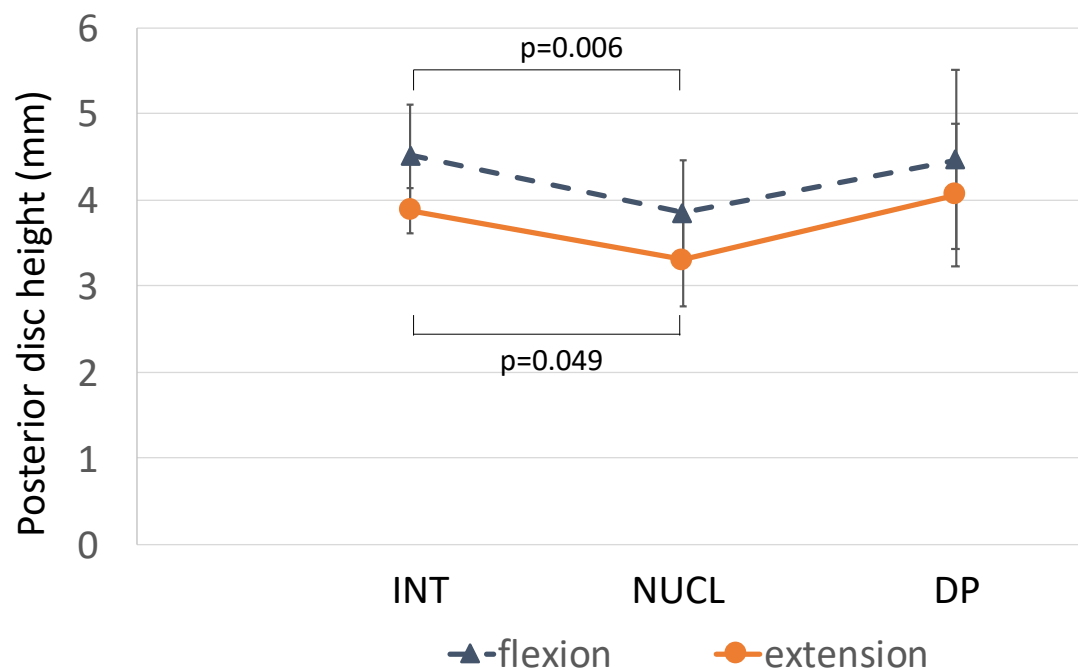


601

602 **Fig. 2** – Workflow of the applied displacement for flexion, extension, and lateral  
603 bending.



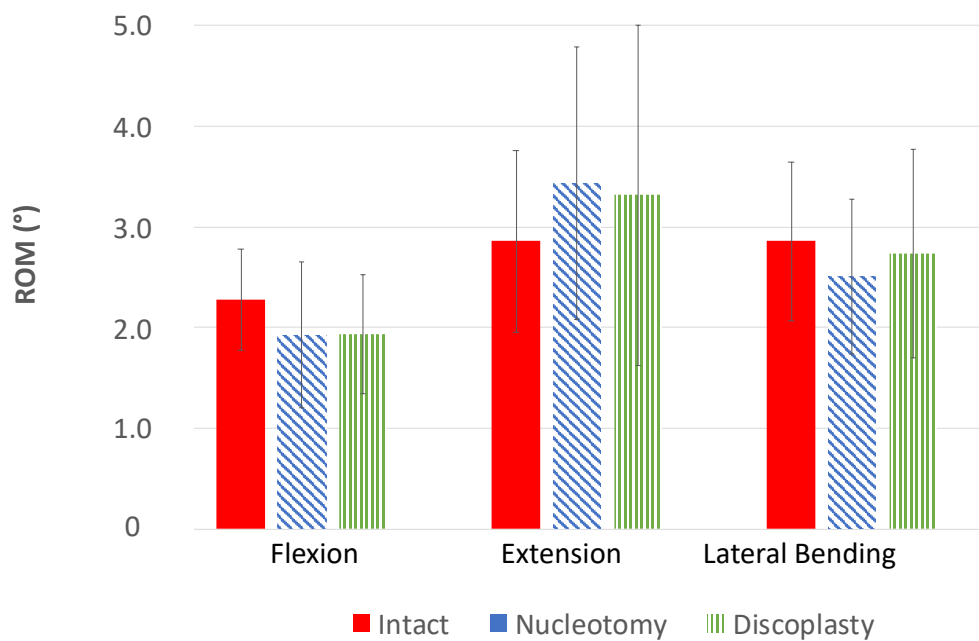
604



605

606 **Fig. 3** – Intervertebral posterior disc height recorded at the peak load in intact  
 607 condition, after nucleotomy, and discoplasty for both motions. Average over all  
 608 specimens and standard deviation were represented (n=10). Normalized data showed  
 609 significant differences in flexion (p=0.11) and extension (p=0.04) between NUCL and  
 610 DP.

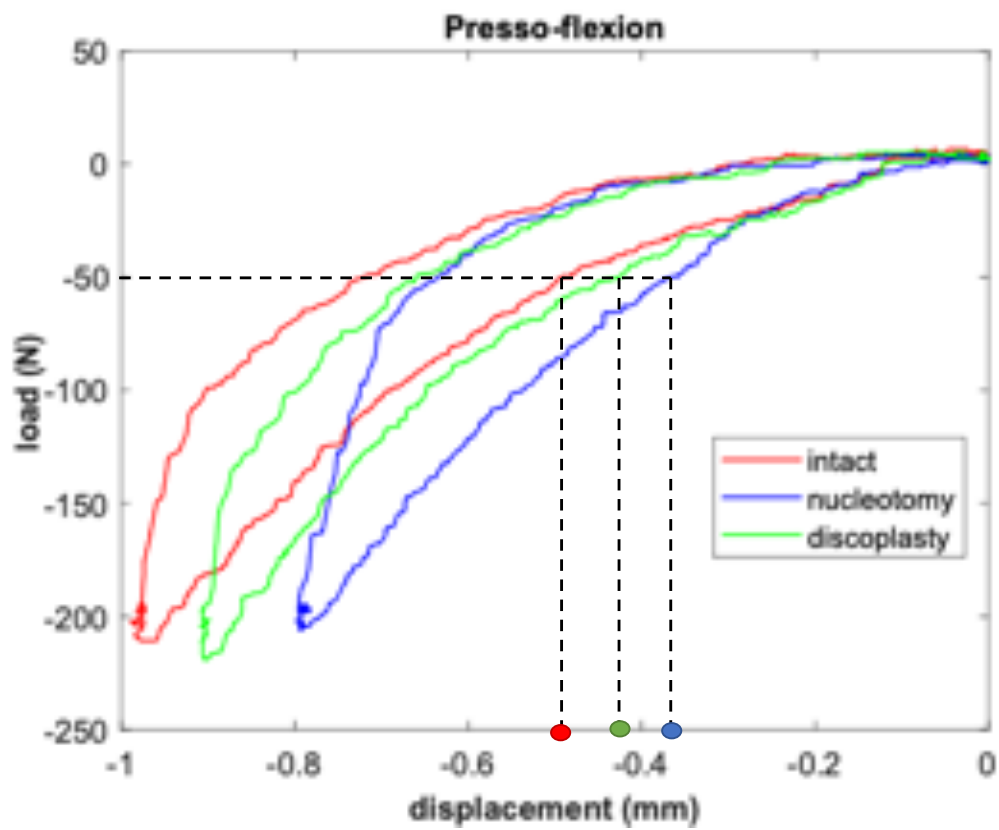
611



612

613 **Fig. 4** – Range of Motion recorded at peak load for flexion, extension and lateral  
614 bending, in all disc conditions. Normalized data were not statistically significant  
615 ( $p>0.1$ ).

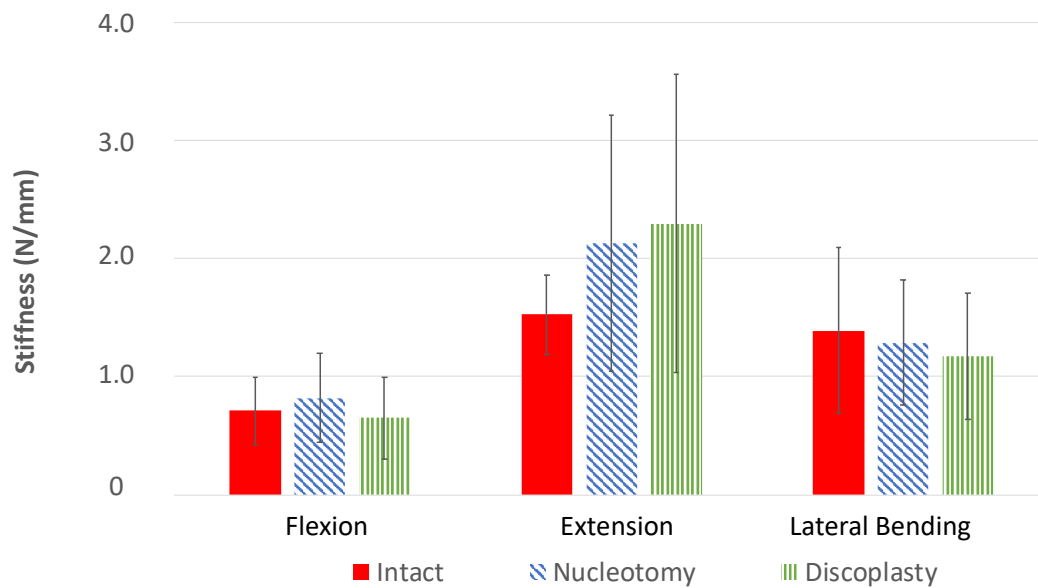
616



617

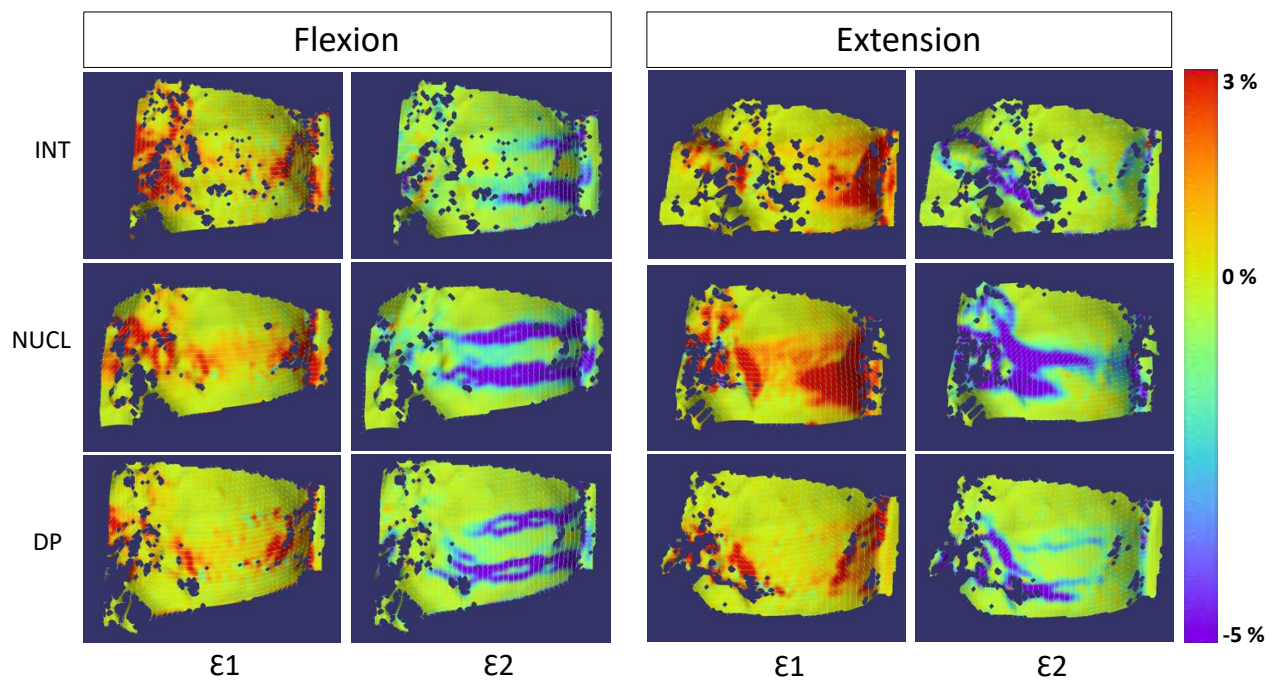
618 **Fig. 5** – Load-displacement curve of a representative specimen tested in extension in  
619 all disc conditions.

620



621

622 **Fig. 6** – Stiffness results in all conditions for all loading configurations. Average was  
623 done over all specimens. Normalized data were not statistically significant ( $p>0.1$ ).



625

626 **Fig. 7** – Showed a typical strain distribution over a specimen surface for a flexion (left)  
 627 and extension (right) bending with first and second principal strains represented for  
 628 each motion.

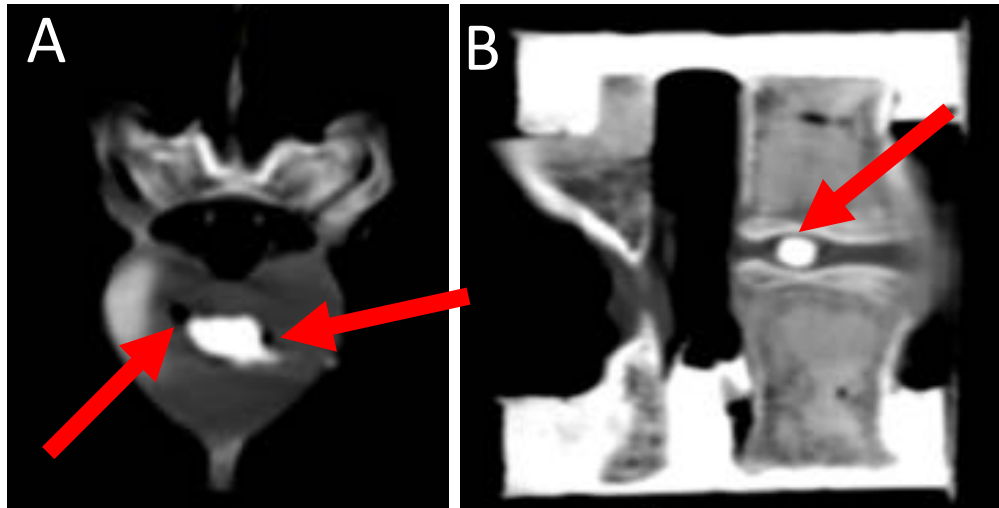
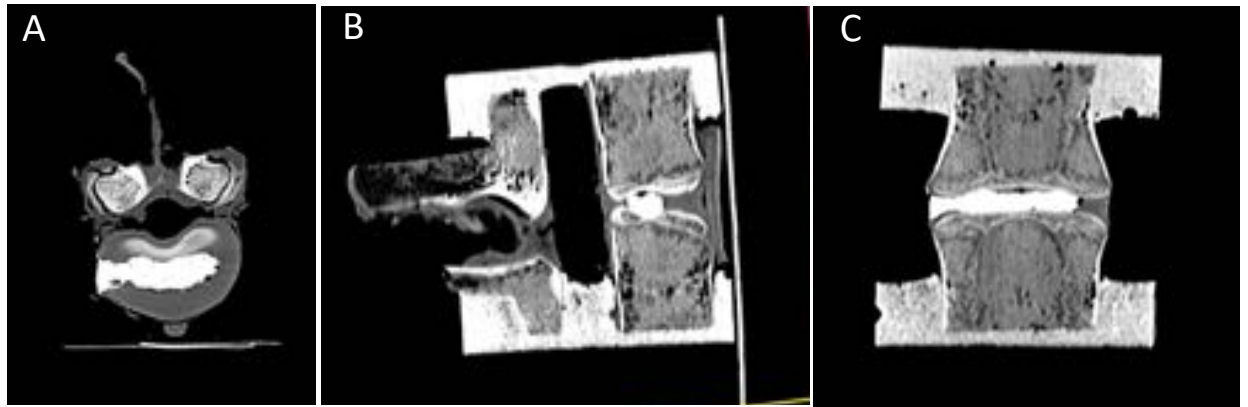


**Fig. 8** –Sub optimal cement distribution. CT scans of porcine specimens in axial (A) and sagittal (B) planes. PMMA did not reach the annulus and the endplates (arrows), leaving vacuum.



635

636 **Fig. 9** – Ideal distribution of the PMMA in the porcine model. CT scan of the porcine  
 637 specimen, A (axial plane) the PMMA filled out the empty space after nucleotomy, B  
 638 (sagittal plane) and C (coronal plane) the PMMA reached the two endplates and adapted  
 639 to the geometry.

## TABLES

*Table 1: Principal strains recorded over the disc surface in Flexion and Extension: The mean and peak (of 10 specimens) are reported for  $\epsilon_1$  and for  $\epsilon_2$ .*

$\epsilon_1$	Flexion		Extension	
	Mean (%)	Peak (%)	Mean (%)	Peak (%)
Intact	1.3±0.6	7.5±2.8	2.2±1.0	11.7±6.0
Nucleotomy	1.3±0.7	10.5±7.1	1.9±0.6	10.1±3.9
Discoplasty	1.0±0.5	8.7±3.5	1.2±0.7	10.0±4.1

$\epsilon_2$	Flexion		Extension	
	Mean (%)	Peak (%)	Mean (%)	Peak (%)
Intact	-2.0±1.2	-17.2±6.1	-0.5±0.4	-8.2±7.5
Nucleotomy	-2.8±1.6	-18.7±8.9	-1.7±1.5	-12.5±10.4
Discoplasty	-1.7±0.9	-16.5±7.3	-0.7±0.8	-13.3±5.3



Table 2: Surface area and volume of the injected cement after segmentation.

Specimen	Spine level	Cement surface area (mm <sup>2</sup> )	Cement volume (mm <sup>3</sup> )
#1	T13-L1*	257.8	282.8
#2	L3-L4	465.8	476.7
#3	T13-L1*	211.6	143.5
#4	L5-L6	623.7	673.9
#5	T13-L1*	712.3	750.3
#6	L3-L4	552.0	608.7
#7	L3-L4	742.2	776.5
#8	L3-L4	557.6	505.4
#9	T15-L1*	592.7	685.0
Mean (SD)	-	524.0 (184.2)	544.8 (215.7)

\* Porcine spines have a variable number of thoracic vertebrae (between 13 and 15).